Experimental Study of Heat Convection From Stationary and Oscillating Circular Cylinder in Cross Flow

H. G. Park
Jet Propulsion Laboratory,
California Institute of Technology
Pasadena, CA 91109

Morteza Gharib
Graduate Aeronautical Laboratories,
California Institute of Technology,
Pasadena, CA 91125

An experimental study is made on the processes of heat transfer from the surface of a forced oscillating cylinder in a crossflow. A range of oscillation amplitude ($A/D=0.1,0.2$), forced oscillation frequency ($0<St_c<1$), and Reynolds number ($Re=550$, 1100, 3500) is covered in water ($Pr=6$). Besides the increase at the natural vortex shedding frequency, large increases in the heat transfer are found at certain superharmonics. By using Digital Particle Image Velocimetry/Thermometry (DPIV/T), the increase in the heat transfer rate is found to correlate inversely with the distance at which vortices roll-up behind the cylinder, i.e., the distance decreases when the heat transfer increases. The cause of the increase is found to be the removal of the stagnant and low heat convecting fluid at the base of the cylinder during the roll-up of the vortices.
[DOI: 10.1115/1.1338137]

Keywords: Convection, Cooling, Cylinder, Enhancement, Entrainment, Experimental, Fluids, Forced Convection, Heat Transfer, Heat Exchangers, Image Processing, Nonintrusive Diagnostics, Recirculating, Separated, Surface, Temperature, Thermal, Unsteady, Vibrating, Vortex, Wakes

Introduction

The process of heat transfer from the surface of a body to the surrounding fluid is of great interest in the field of thermo-fluid mechanics. This process is of technological importance in the design of heat exchanger devices such as cooling or heating systems. One body shape of particular importance is a bluff body, and the most commonly studied is the circular cylinder. Despite its simple shape, a circular cylinder generates a wake which is dynamically complex. The most essential parameter which characterizes the wake of a smooth circular cylinder is the Reynolds number, $Re=U_\infty D/\nu$, where U_∞ is the freestream velocity, D is the diameter, and ν is the kinematic viscosity. Below $Re\approx5$, the wake is steady and the boundary layer remains attached. Above $Re\approx5$, the boundary layers on top and bottom separate (Taneda [22]) which gives rise to a pair of steady symmetric vortices in the wake. The vortices become elongated as the Reynolds number is increased until the symmetry is broken at $Re\approx40$, where the wake becomes unsteady, and the Karman vortices appear downstream. Above $Re\approx90$, the wake is characterized by alternate shedding of vortices at the top and bottom of the cylinder with opposite signs of vorticity; a process termed ''vortex shedding.'' While unsteady, the flow remains laminar and two-dimensional until $Re\approx180$ (Williamson [24]), above which the wake becomes three-dimensional and ''turbulent.'' At above $Re\approx1000$, the separated shear layers, which roll-up to form the vortices, become turbulent, and the wake progressively grows more turbulent. Finally, above $Re\approx200{,}000$, or the ''critical'' Reynolds number, the boundary layer on the cylinder surface becomes turbulent, and the wake narrows to produce a large reduction in drag. A review of this Reynolds number region is given by Bearman [1]. Beyond this Reynolds number, little is known about the structure of the wake of a circular cylinder.

Thus by varying the Reynolds number, a rich set of flow patterns is observed, but even more wake patterns are observed by forced oscillation of the cylinder. Under forced transverse oscillations, various vortex shedding patterns are possible by varying the oscillation frequency and amplitude. An extensive review of the wake patterns is given by Williamson and Roshko [24], and some possible patterns are shown in Fig. 3(*a–b*) in their paper. At oscillation frequencies below the vortex shedding frequency of a stationary cylinder, the vortices may be shed and paired in various different ways. At oscillation frequencies above the vortex shedding frequency of a stationary cylinder, the cylinder may shed small vortices which then coalesce into large vortices. For small amplitudes ($A/D<0.5$), the large vortices may recover to the Karman vortex street farther downstream. The wake patterns at high oscillation frequencies have been studied by Ongoren and Rockwell [17] who reported that the large vortices, which form in the near wake ($x/D<5$) by the coalescence of smaller vortices, shed at or near the vortex shedding frequency of a stationary cylinder. At the super-harmonic frequencies, i.e., multiples of the vortex shedding frequency of a stationary cylinder, they observed organized vortex shedding patterns where a pair of small vortices are shed for each cycle of cylinder oscillation and coalesce with nearby vortices to form the large vortices.

It is intuitive to believe that oscillating a cylinder in a fluid will increase its heat transfer from its surface. Martinelli and Boelter [12] measured that the heat transfer from the surface of a cylinder is increased up to 500 percent compared to that of free convection by oscillating it in water. Surprisingly, for the case of forced convection over a circular cylinder ($5000<Re<25{,}000$), Sreenivasan and Ramachandran [21] found no appreciable increase in heat transfer for large forced transverse oscillation amplitudes of $A/D=0.43$ and 3.7 as compared to that of a stationary cylinder. However, the oscillation frequencies they concentrated on were well below the vortex shedding frequency of a stationary cylinder. A different study by Kezios and Prasanna [11] ($5500<Re<14{,}000$) focused on oscillation frequency corresponding to the vortex shedding frequency of a stationary cylinder. The study found that the surface heat transfer increased by approximately 20 percent, even for small amplitudes ($0.02<A/D<0.075$) when the oscillation frequency matched the vortex shedding frequency. It

Contributed by the Heat Transfer Division for publication in the JOURNAL OF HEAT TRANSFER. Manuscript received by the Heat Transfer Division January 3, 2000; revision received, May 17, 2000. Associate Editor: Bau.

was noted that the increase in heat transfer could not be accounted for by the relative increase in the freestream velocity due to the transverse motion of the cylinder. Saxena and Laird [20] found that a large increase (40 percent to 60 percent) in heat transfer occurs in water as the forced oscillation frequency approached the vortex shedding frequency of a stationary cylinder for large oscillation amplitudes ($0.89<A/D<1.99$) at Re=3,500. The maximum frequency reached was 0.8 times the shedding frequency. More recently, Karanth et al. [9] conducted a computational study at Re=200 where increases of 1.2 percent and 3 percent in the surface heat transfer were observed for forced transverse oscillations amplitudes of $A/D=0.25$ and 0.5, respectively. Cheng and Hong [5], in another computational study at Re=200, observed that the heat transfer increased 1.6 percent, 3.9 percent, 7.5 percent, and 12.5 percent for $A/D=0.14$, 0.3, 0.5, and 0.7, respectively. Following their computational study, Cheng et al. [4] measured increases in the surface heat transfer from 3 percent to 30 percent for $A/D=0.138$, 0.314, 0.628 at Re=200, 500, and 1000 when the cylinder was forced to oscillate at the vortex shedding frequency of a stationary cylinder. A new study by Gau et al. [8] found increase in the heat transfer up to 50 percent for $A/D=0.064$ at Re=1600 in air for an oscillating cylinder. The study covered small amplitudes, $A/D=0.016$, 0.032, and 0.064 and Re range of 1600, 3200, and 4800. For Re=1600, the cylinder was oscillated to three times the natural vortex shedding frequency, and they found even higher increase (70 percent) in the heat transfer rate.

The previous authors have cited the phenomenon of ''lock-in'' or the synchronization of the vortex shedding with the mechanical oscillation of the cylinder as the reason for the increase in the surface heat transfer. When the vortex shedding becomes synchronized with the mechanical oscillation, a pair of vortices is always shed for each cycle of cylinder oscillation. However, it has never been fully explained why this synchronization leads to higher surface heat transfer. In addition, Cheng et al. [4] noticed that past the synchronization frequency, the heat transfer continued to increase for large amplitudes ($A/D=0.626$), decreased then increased for medium amplitudes ($A/D=0.314$), or returned too close to the value of the stationary cylinder for small amplitudes ($A/D=0.138$). (See Fig. 6 of Cheng et al. [4]) The study stopped at 1.5 times the synchronization frequency, and the increase in the heat transfer for larger oscillation amplitudes at higher frequencies was attributed to the ''turbulence'' effect. The ''turbulence'' effect was left unclear and is presumed to be connected to some unsteadiness in the wake or boundary layer of the cylinder.

Recent flow visualization study of Gau et al. [8] showed that the vortices roll-up close to the cylinder when the oscillation frequencies are one and three times that of the natural vortex shedding frequency for $0.016<A/D<0.064$. This result hints that perhaps coherent motions the vortices, i.e., organized structure of the wake, is responsible for the rise in the heat transfer rate at certain oscillation frequencies. Thus a comprehensive set of experiments is carried out to study the relationship between the heat transfer and the wake behind the cylinder. First, a study is made of the overall heat transfer of a forced oscillating heated cylinder near the natural vortex shedding frequency, similar to previous studies. In addition, the heat transfer characteristics of a forced heated cylinder is examined all the way up to five times the natural shedding frequency where new findings are uncovered. Second, a study is made of the wake structure at selected frequencies and amplitudes to address the primary cause of the increased heat transfer near the natural shedding and other frequencies.

Experimental Setup and Procedure

Experimental Setup. A schematic of the water tunnel facility where the experiments were conducted is shown in Fig. 1. The cross-sectional dimensions of the test section were 15.2 cm wide and 15.2 cm high. The tunnel was operated by a pair of pumps and had a speed range of 3 to 50 cm/s. The temperature of the flow through the test section could be raised by a bank of staggered heating rods in the inlet pipe to the diffuser section of the tunnel and could be lowered by a re-circulating chiller (Neslab RTE-110) at the downstream section of the tunnel. Using a closed-loop temperature controller (Tronac PTC-41), the mean freestream temperature could be maintained to within ± 0.02°C at a flow speed of 5 cm/s or within ± 0.01°C at a flow speed of 40 cm/s.

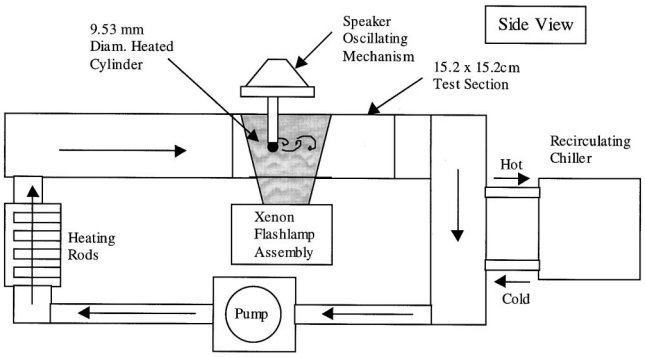

Fig. 1 Schematic of water tunnel facility

The test cylinder was an electrically heated rod of diameter 9.53 mm (Watlow Firerod). The electric heating element was protected by an outer sheath made from Incoloy alloy. A J-type thermocouple, which gave an estimate of the cylinder temperature, was embedded in the core of the cylinder at mid-span. The cylinder was heated by a constant DC voltage power supply (Kepco BOP 50-4M), and its temperature was measured by a thermocouple thermometer (Omega HH21) which had a resolution of ± 0.1°C. The cylinder had a thermal boundary condition of constant integrated heat flux over the surface. The cylinder was mounted horizontally to a transverse oscillating mechanism by two vertical hollow supports at the ends of the cylinder. The electrical and thermocouple leads were passed through the hollow supports from the cylinder to the power supply and thermocouple thermometer, respectively. The supports were thermally insulated from the cylinder by a layer of silicone. The disturbance to the flow was minimized by placing the supports outside of two flat end plates that had rounded leading edges. The distance between the two end plates was 12.1 cm, and thus the effective aspect ratio (L/D) of the cylinder was 13.

The oscillating mechanism was a 15 cm cone speaker in which the cone was stiffened by a circular thin-aluminum plate. The plate provided torsional stiffness to the cone and kept the cylinder level with respect to the bottom of the tunnel. The speaker was driven by a feedback amplifier that was fed a sinusoidal signal from a multi-wave generator (HP 3314A). With the cylinder mass, the speaker was capable of generating sinusoidal motion amplitude of 4 mm peak-to-peak from 0 to 10 Hz. The actual displacement of the cylinder was measured by an optical transducer (photo-detector grid) which generated a voltage proportional to the displacement of the laser diode mounted on the cylinder oscillating mechanism.

Velocity and Temperature Measurements

The freestream velocity measurements were made using a single component Laser Doppler Anemometer (LDA) placed several diameters upstream of the test cylinder. The velocity and temperature measurements in the wake were made using Digital Particle Image Velocimetry/Thermometry (DPIV/T). The details of DPIV/T are found in Park [18], Dabiri and Gharib [6], and Willert and Gharib [23]. The flow was seeded with encapsulated TLC particles and was illuminated by a reflector assembly which produced a sheet of light at the center of the test section. The light reflector assembly was a mirror surfaced elliptical cylinder with a

thin slit on top. The light, which was produced by two 25 cm long xenon flashtubes located at the foci of the ellipse, escaped through the slit and was collimated by two lenses to form a light sheet of 2–3 mm thickness. Each flashtube was fired at 15 Hz with a flash duration of 150 μs and had an energy release of 8 J. Alternate firing of the flashtubes synchronized with the 30 Hz frame rate of the video camera.

The flow was imaged from the side of the water tunnel using a 3-CCD color camera (Sony DXC-9000) which has a standard set of NTSC R, G, and B color filters. The camera, which was placed approximately 2 m from the test section, imaged an area of 60 mm wide by 50 mm high at the mid-span of the test section. The flow was seeded with 40 μm diameter thin-walled encapsulated TLC particles (Hallcrest BM40C26W20) which had thermal response time of 4 ms (Dabiri and Gharib [6]). The response time was much smaller than the expected time scale of the vortex shedding ($\approx$600 ms). The flow was illuminated from the bottom of the test section by a xenon white light sheet of 2–3 mm thickness, and the images were digitized to a real-time digital video recorder with 8-bit resolution per RGB channel (24-bit total).

The velocity distribution was measured using standard DPIV technique. While temperature distribution of the wake was obtained using DPIV/T, only the velocity measurements are presented for the purposes of this paper. The heat transfer rate was not derived from the temperature distribution of the wake. Instead, the rate was measured directly from the thermocouple and heat input measurements as described in a later section.

Phase Averaging Methodology

For each of the frequency and amplitude, the structure of the wake was studied by phase averaging the DPIV/T velocity data. The phase averaged statistics were generated from 1000 pairs of image, corresponding to 1000 instantaneous velocity fields. This number represents roughly 95 vortex shedding cycles. For the forced oscillating cases, there was no ambiguity in phase since the phase averaging was synchronized with the mechanical motion of the cylinder. Depending on the case, the displacement signal was divided into either 6 or 12 evenly spaced phases. However, an ambiguity was encountered in the phase for the stationary cylinder since the period of the shedding varied slightly for each cycle. This ambiguity has been encountered by both Cantwell and Coles [3] and Matsumura and Antonia [13] who had to adjust slightly the period of each vortex shedding cycle to compute the phase average correctly. Similarly, the period of each vortex shedding cycle was adjusted in computing the phase average quantities.

For the stationary cylinder or a case in which the vortex shedding is not synchronized with the mechanical oscillation of the cylinder, a reference signal from which the phase of the vortex shedding can be determined is needed. Cantwell and Coles [3] used the signal from a static pressure tap on the surface of the cylinder 65 deg from the forward stagnation point of the cylinder, while Matsumura and Antonia [13] used the signal from a hot-wire just outside of the wake. Others have used the lift signal as the reference signal (Karniadakis [10]), but any clean signal generated by the vortex shedding process is sufficient. For this study, the vertical velocity (u_y) at the location of maximum fluctuation level on the centerline of the wake was used as the reference signal. The maximum u_y fluctuation level occurs just downstream the region where the vortices roll-up, and the signal there is both clear and large in magnitude. The period of each shedding cycle was determined by measuring the time between consecutive zero crossings of the u_y signal, and each period was divided into 12 evenly spaced phases.

Nusselt Number Versus Oscillation Frequency

Experimental Conditions. The average heat transfer from the surface of a cylinder undergoing forced oscillation was measured for three different Reynolds numbers of 550, 1100, and 3,500 based on a freestream temperature of 25.8°C. The Prandtl number, Pr, of water at this temperature is 6. The cylinder was heated with constant power inputs of 45.5, 58.4, and 90.9 W for Re=550, 1100, and 3500, respectively. The ratio between the Grashof number and the square of the Reynolds number, Gr/Re^2, which is a measure of the buoyancy effect, was low enough (0.01) to not affect the wake structure.

The measurements were made at two amplitudes, $A/D=0.1$ and 0.2. The range of Strouhal frequency of the cylinder, St_c, was from 0 to 0.95 for Re=550 and 1,100. The Strouhal number of the cylinder is defined as $f_cD/U\infty$ where f_c is the cylinder oscillation frequency. The ranges in physical frequency unit were from 0 to 5.6 Hz for Re=550 and from 0 to 11.4 Hz for Re=1,100. For Re=3500, the range of St_c was from 0 to 0.35, corresponding to a range in physical frequency from 0 to 13.4 Hz. The maximum frequency at this Reynolds number was limited by the mechanical driving mechanism which could not exceed 14 Hz.

Nusselt Number Calculations

The Nusselt number, defined as

$$\mathrm{Nu}=\frac{hD}{k},$$

where h is the average convection heat transfer coefficient, and k is the thermal conductivity of the fluid medium, is computed from the estimate of the average surface temperature of the cylinder and the input power. Because the Biot number, defined as

$$\mathrm{Bi}=\frac{hD}{k_c},$$

where k_c is thermal conductivity of the cylinder, is of the order unity, the approximation that the temperature at the surface, T_c, is the same as the temperature at the core, T_{tc}, cannot be made. Therefore, a first order approximation is made to estimate the surface temperature from the core temperature as measured by the embedded thermocouple (T_{tc}).

The procedure is as follows. We assume that the temperature varies only in the radial direction and that the cylinder is composed of a uniformly heated inner shell and an unheated outer shell (Fig. 2). If we assume uniform material properties, the steady-state temperature distribution in the inner shell is then given by the heat equation in radial coordinates:

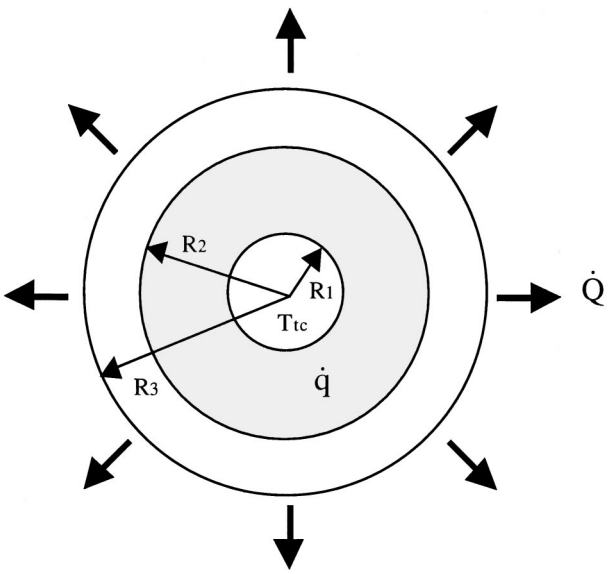

Fig. 2 Layout of the cylinder

$$\frac{\partial^2 T}{\partial r^2}+\frac{1}{r}\frac{\partial T}{\partial r}+\frac{\dot{q}}{k}=0 \quad (R_1 \leqslant r \leqslant R_2), \tag{1}$$

where $\dot{q}$ is the power input per unit volume, or:

$$\dot{q}=\frac{\dot{Q}}{\pi(R_2^2-R_1^2)L}, \tag{2}$$

where $\dot{Q}$ is the total power input, L is the length of the cylinder, R_1 is the radius at which the thermocouple is located, and R_2 is the outer radius of the inner shell. The steady-state temperature distribution in the outer shell is given simply by

$$\frac{\partial^2 T}{\partial r^2}+\frac{1}{r}\frac{\partial T}{\partial r}=0, \quad (R_2 \leqslant r \leqslant R_3). \tag{3}$$

The boundary conditions for these equations are:

$$T(R_1)=T_{tc}, \tag{4}$$

$$-k_{CO}\left.\frac{\partial T}{\partial r}\right|_{r=R3}=h(T_c-T_\infty)=\frac{\dot{Q}}{2\pi R_3 L}, \tag{5}$$

where k_{CO} is the thermal conductivity of the outer shell, and R_3 is the outer radius of the cylinder. The matching condition is at R_2 where the temperatures of the outer and inner shells must be equal. Solving Eqs. (1) and (3) with the appropriate boundary conditions, the temperature at the surface, T_c, is given by

$$T_c=T_{tc}-\frac{\dot{Q}}{2\pi L}\left[\frac{1}{k_{CO}}\ln\left(\frac{R_3}{R_2}\right)+\frac{1}{k_{CI}}\left(\frac{1}{2}-\frac{R_2^2}{R_2^2-R_1^2}\ln\left(\frac{R_2}{R_1}\right)\right)\right], \tag{6}$$

where k_{CI} is the thermal conductivity of the inner shell. From Eqs. (5) and (6), we can compute the convection heat coefficient, where

$$h=\frac{\dfrac{\dot{Q}}{2\pi R_3 L}}{\left\{\begin{array}{c}(T_{tc}-T_\infty)\\ -\dfrac{\dot{Q}}{2\pi L}\left[\dfrac{1}{k_{CO}}\ln\left(\dfrac{R_3}{R_2}\right)+\dfrac{1}{k_{CI}}\left(\dfrac{1}{2}-\dfrac{R_2^2}{R_2^2-R_1^2}\ln\left(\dfrac{R_2}{R_1}\right)\right)\right]\end{array}\right\}}. \tag{7}$$

From h, we can then compute the Nusselt number.

The computed Nusselt number inherently has a level of uncertainty because the surface temperature of the cylinder is not truly uniform. The temperature at the base of the cylinder is typically higher than at the forward stagnation point. This was confirmed by intrusive measurements using a thermocouple at various circumferential locations around the cylinder. The temperature gradients in the radial direction were found to be roughly three times higher than the circumferential direction. To quantify this error, a detailed two-dimensional finite element simulation was carried out using circumferential distribution of Nusselt number from Gau et al. [8]. The results show that the bias error in Nusselt number using the one-dimensional approximation instead of two-dimensional is roughly 25 percent. However, the relative uncertainty, i.e., uncertainty between two measurements, is smaller at 10 percent and is the quantity of interest in this paper. This is discussed further in the error analysis section.

Results

The plots of normalized Nusselt number versus oscillation frequency are shown in Figs. 3 and 4 for $A/D=0.1$ and 0.2, respectively. The Nusselt number is normalized by the respective stationary values at each Reynolds number. The stationary Nusselt number values for Reynolds number 550, 1100, and 3500 are 19.5, 24.8, and 56.0, respectively. For each Reynolds number and

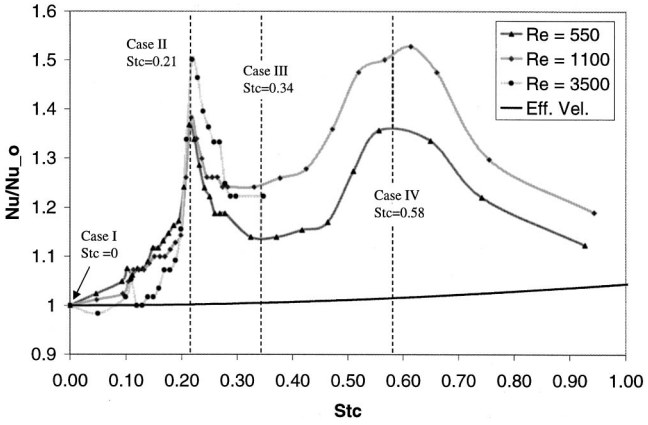

Fig. 3 Normalized surface heat transfer as function of oscillation frequency for $A/D=0.1$

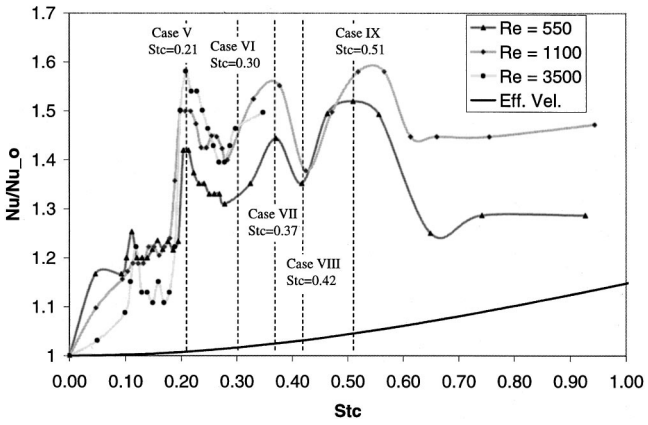

Fig. 4 Normalized surface heat transfer as function of oscillation frequency for $A/D=0.2$

oscillation amplitude, a peak near $St_c \approx 0.21$ is observed. These peaks are associated with the synchronization of the vortex shedding with the mechanical oscillations. This phenomenon has been well documented by many previous researchers starting from Kezios and Prasanna [11]. For each Reynolds number, higher oscillation amplitudes results in higher Nusselt number at this frequency as noted by previous researchers (Kezios and Prasanna [11]; Cheng et al. [4]).

The locations of all of the peaks appear to be correlated with the amplitude of oscillation. The figures show that the locations of the peaks and valleys are nearly coincident for given amplitude, irrespective of the Reynolds number. For $A/D=0.1$, there is a broad valley from $St_c \approx 0.3$ to ≈ 0.45, and a broad peak at $St_c \approx 0.6$ with roughly the same height as the peak at $St_c=0.21$. For $A/D=0.2$, there are valleys at $St_c \approx 0.3$ and 0.4, and two peaks at $St_c \approx 0.35$ and ≈ 0.55.

Discussion

While it has been well documented that there is an increase in the Nusselt number at the synchronization frequency ($St_c \approx 0.2$), the increases in the Nusselt number at other frequencies have not been well documented. The results of this study show that the Nusselt number does not increase or decrease monotonically past the synchronization frequency ($St_c \approx 0.2$) but has definite peaks and valleys. As will be seen in the following sections, the peaks are associated with certain modes of the wake. The increase at $St_c \approx 0.6$ for $A/D=0.1$ is associated with a mode at three times the natural shedding frequency, whereas the increases seen at $St_c \approx 0.35$ and 0.55 for $A/D=0.2$ are associated with modes at twice

and three times the natural vortex shedding frequency, respectively. At the higher amplitude ($A/D=0.2$), the mode frequencies appear to have shifted slightly away from exact multiples of the fundamental synchronization frequency.

The increase in the Nusselt number cannot be simply accounted for by the ''effective'' velocity of the cylinder due to added velocity from the oscillatory motion of the cylinder. Following Sreenivasan and Ramachandran [21], the effective velocity, V_e, is defined as:

$$V_e=\sqrt{U_\infty^2+V_v^2}, \tag{8}$$

where

$$V_v=\frac{2\pi fA}{\sqrt{2}}, \tag{9}$$

is the RMS velocity of the oscillation. For a stationary cylinder, the MacAdams relation (MacAdams [14]) predicts the Nusselt number as function of the Reynolds number ($100<\mathrm{Re}<4000$) or the freestream velocity as:

$$\mathrm{Nu}\propto \mathrm{Re}^{0.475}\propto U_\infty^{0.475}. \tag{10}$$

Substituting V_e into Eq. (7), the Nusselt number as function of oscillation frequency and freestream velocity becomes:

$$\mathrm{Nu}(A,f_c,U_\infty)\propto(U_\infty^2+2\pi^2f_c^2A^2)^{0.475}. \tag{11}$$

This relationship is plotted as the solid curves in Fig. 3 and 4. As noted by previous researchers (Cheng et al. [4]), the relation in Eq. (11) cannot account for the increase in the Nusselt number for the oscillation frequencies of interest.

The trends in Figs. 3 and 4 are actually consistent with those observed by Cheng et al. [4] and Gau et al. [8]. Chen et al. [4] observed that for $A/D=0.138$, the Nusselt number decreased and remained low past $\mathrm{St}_c\approx0.2$, while at $A/D=0.314$, the Nusselt number first decreased then began to increase again. Since they did not measure the Nusselt number beyond 1.5 times the shedding frequency ($\mathrm{St}_c\approx0.30$), they were likely observing a decrease associated with a valley from $\mathrm{St}_c\approx0.3$ to ≈0.45 for $A/D=0.134$, and an increase associated with a peak at $\mathrm{St}_c\approx0.35$ for $A/D=0.314$. They attributed the rise at $A/D=0.314$ past St ≈0.3 to the ''turbulence'' effect. They did not precisely define what the ''turbulence'' effect was, although it is inferred from their paper that it is associated with some unsteady (incoherent) motion of the wake or the boundary layer.

Further information about the wake comes from Gau et al.[8] who found a rise in the heat transfer for $\mathrm{St}_c\approx0.6$ or 3 times the shedding frequency for $A/D=0.064$. Their flow visualization results gave an impression that organized structures in the wake may be responsible for the increase in the heat transfer. Therefore, a detailed DPIV/T study of the wake is presented to clarify the connection between the wake structure and the rate of heat transfer.

DPIV/T Study

Experimental Conditions. A detailed DPIV/T study of wake was carried out at Reynolds number of 610. The freestream temperature was 25.8°C, and the cylinder was heated with a constant power input of 63.8 W. The wake velocity-temperature field measurements were made for two different amplitudes ($A/D=0.1$ and 0.2) at frequencies corresponding to peaks and valleys of the heat transfer versus oscillation frequency curve in Figs. 3 and 4. A total of nine cases, denoted by Roman numerals I through IX, are presented at frequencies and amplitudes shown in Figs. 3 and 4.

Roll-up Distance Versus Heat Transfer. The most important result from the DPIV/T study is the connection between the length of the mean wake bubble, i.e., length of the recirculation bubble, and the surface heat transfer. Figure 5 shows that there is a strong correlation between the wake bubble length and the overall Nusselt number. There is, however, a dependence on oscillation amplitude. The wake bubble length is computed by averaging the velocity field and locating the closure point of the recirculation bubble. For example, the wake bubble length is much shorter for the forced oscillated cylinder, Case II, ($x/D=1.3$) than for the stationary cylinder, Case I, ($x/D=2.5$) which has much lower heat transfer rate. For all of the high heat transfer cases, Case II, IV, V, VII, and IX, the wake bubble lengths are short, $x/D<1.5$, while for all of the low heat transfer cases, Case I, III, VI, and VIII, the lengths are long, $x/D>1.9$ (Fig. 5).

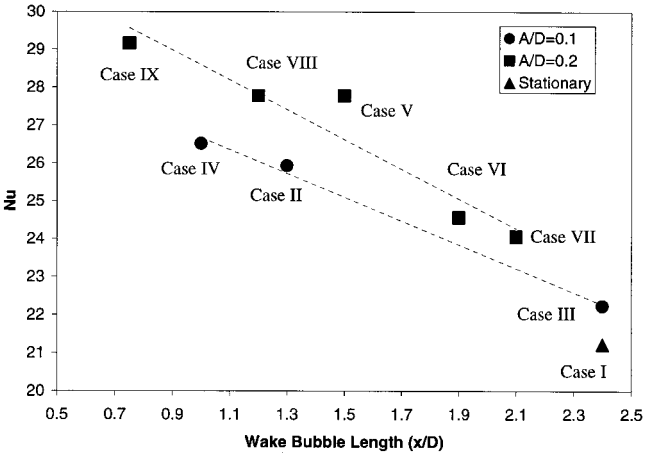

Fig. 5 Nusselt number versus length of the mean wake bubble (formation length)

The length of the wake bubble is a quantitative measure of the downstream distance at which the wake vortices roll-up. Thus the reason behind the increased heat transfer when the vortices roll-up close to the cylinder is that the vortices are able to scrub away the hot fluid at the base of the cylinder. For Case I (stationary cylinder), there is a region of stagnant fluid just behind the cylinder which does not convect any heat away from the base of the cylinder. Figure 6 shows the closest approach that a vortex makes during its roll-up. The vortex is sufficiently far away that the fluid near the base of the cylinder remains stagnant and does not carry away any heat. In the high heat transfer cases, this region of stagnant fluid is non-existent. As an example, Fig. 6 shows the closest approach that a vortex makes during its roll-up in Case II. The vortex is close enough to induce flow around the base of the cylinder and carry away heat from the base. While the local Nusselt number was not measured in this study, and thus the increase in the heat transfer at the base of the cylinder could not be directly verified, it is strongly believed that the heat transfer increases at the base when the vortices scrub away the normally stagnant and non-heat convecting fluid away from the cylinder at the base. The overall heat transfer thus increases when the heat transfer rate at the normally low region (Eckert and Soehngen [7]) is increased.

Intuitively it is interesting to correlate the length of the wake bubble with the rate of surface heat transfer. However, the heat transfer cannot be a simple function of the wake bubble length because the length can grow or shrink as function of only the Reynolds number. It has been observed that the length of the wake bubble, or the ''formation length'' of the vortices, increases for roughly $200<\mathrm{Re}<1500$ (Bloor [2]). For a cylinder with ''high'' aspect ratio ($L/D>50$), the length of the wake bubble increases from $x/D=1.6$ to 2.2 ($\approx$40 percent increase) from Reynolds number 500 to 1000 for a stationary cylinder (Noca et al. [15]). The Nusselt number may also increase in this span of Reynolds number by $\approx$40 percent (MacAdams [14]). Since the trends are opposite to those of the forced oscillating cylinder (increase in wake bubble length results in decreased heat transfer), the Reynolds number, not the wake bubble length, must be the essential parameter in determining the heat transfer from a stationary cylinder.

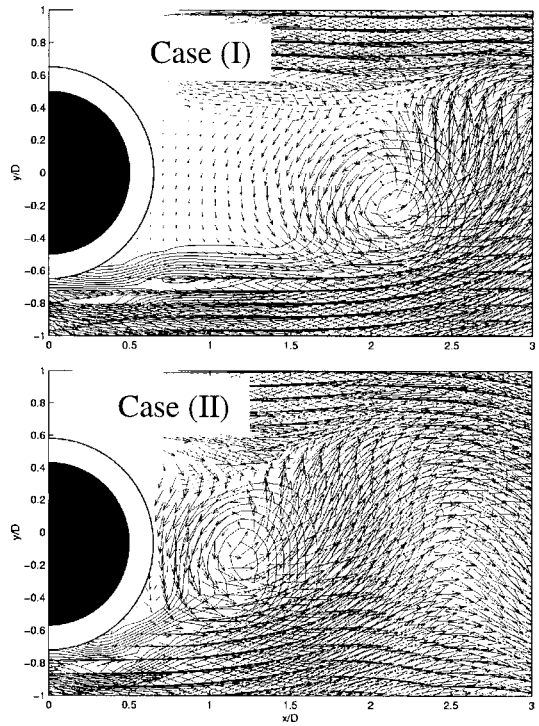

Fig. 6 Stagnant and non-heat convecting fluid near the base of the cylinder for Case (I), and vortices scrubbing away fluid near the base of the cylinder for Case (II). Note the close roll-up of the vortex and large velocity near the base of the cylinder in Case (II) as compared to Case (I). Note: the contours are lines of constant vorticity.

When the cylinder is in forced oscillation, the wake bubble length, not the ''effective'' Reynolds number or freestream velocity (Eq. 11), appears to be the essential parameter in correlating the heat transfer. These effects must be kept in mind when examining the trend between the wake bubble length and Nusselt number as shown in Fig. 5.

The increase in the heat transfer may be also correlated with the increase in the vorticity flux through a surface normal to the wake centerline as shown in Fig. 7. The measured vorticity flux is the amount of surface normal vorticity (ω_z) passing in the streamwise direction through a surface below the wake centerline at $x/D = 0.8$, i.e., the location of the lower shear layer. The most likely reason why the Nusselt number correlates so well with the vorticity flux is that the amount of vorticity a shear layer contains may have direct influence the formation length, i.e., length of the mean wake bubble. It is observed that the larger the amount of vorticity flux, the shorter the length of the bubble. This is consistent with the ''free-streamline'' or ''cavity'' theory (Roskho [19]) which predicts that the bubble length will decrease if the vorticity flux is increased. Hence, a shorter bubble length implies more closely rolled-up vortices which are more effective in transporting away the non-heat convecting fluid at the base of the cylinder. The correlation between the vorticity flux and the length of the mean wake bubble is shown in Fig. 8.

Structure of the Wake. The observation of a short wake bubble length, or a roll-up of the vortices close to the cylinder, always coincides with the synchronization of the wake with some integer fraction ($1/n$, $n=1,2,3$) of the mechanical oscillation frequency. Regardless of the oscillation frequency, the frequency of the large-scale vortex shedding remains near $St=0.2$ (Ongoren and Rockwell [17]). When the frequency of oscillation approaches some multiples of the large-scale vortex shedding frequency, the wake pattern becomes synchronized with the cylinder oscillation,

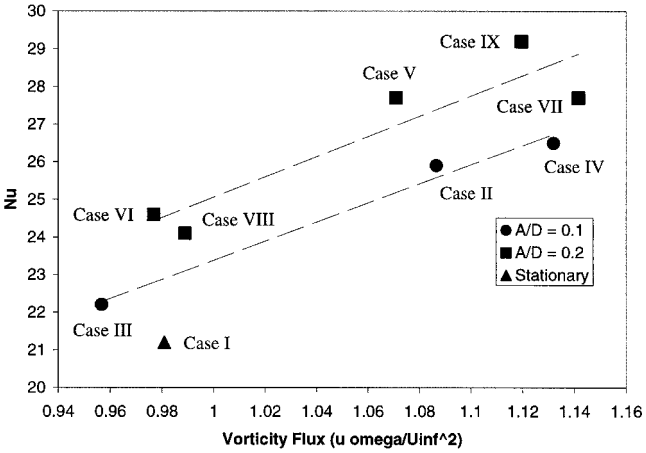

Fig. 7 Nusselt number versus mean total vorticity flux of the lower shear layer at $x/d=0.8$

and this may result in the roll-up of the vortices very close to the cylinder. In Cases II and V, the wake is synchronized with the mechanical oscillation frequency since the wake and oscillation frequencies match. For other frequencies that are multiples or close to multiples of the large-scale vortex shedding frequencies, period doubling (case VII) and period tripling (cases IV and IX) are observed with respect to the cylinder oscillation period. This phenomenon of period doubling and tripling has been observed by Ongoren and Rockwell [17] through flow visualization in water (hydrogen bubble technique) for cylinders of various shapes. For a wedge shaped cylinder, they observed the formation of one small vortex per side (top and bottom) for each oscillation of the cylinder when the oscillation frequency was an integer multiple, n, of the large-scale vortex shedding frequency. The n distinct vortices merged downstream to form the large-scale vortices which then shed at a much lower frequency ($1/n$ of the oscillation frequency). The merging process is shown in Fig. 11 of Ongoren and Rockwell [17]. Similar observations are made in this study, except that merging appears to occur much closer for the case of the circular cylinder, especially for Case IV and IX (i.e., $n=3$). Figure 9 shows the sequence of phase averaged vorticity fields for Case IV. Ongoren and Rockwell [17] observed that oscillating the cylinder three times the natural shedding frequency generated three distinct vortices per side, of which the first two merged some distance ($x/D\approx 2.5$, where D is the side length of a 60 deg wedge) downstream followed by a merger of the third vortex with the first two at $x/D\approx 4$. In this study (circular cylinder as opposed to a wedge), three distinct vortices are not observed. Instead, one large vortex

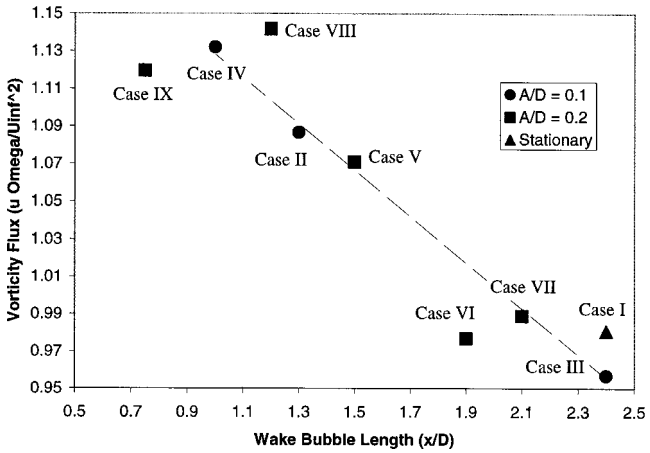

Fig. 8 Vorticity flux versus the length of the mean wake bubble

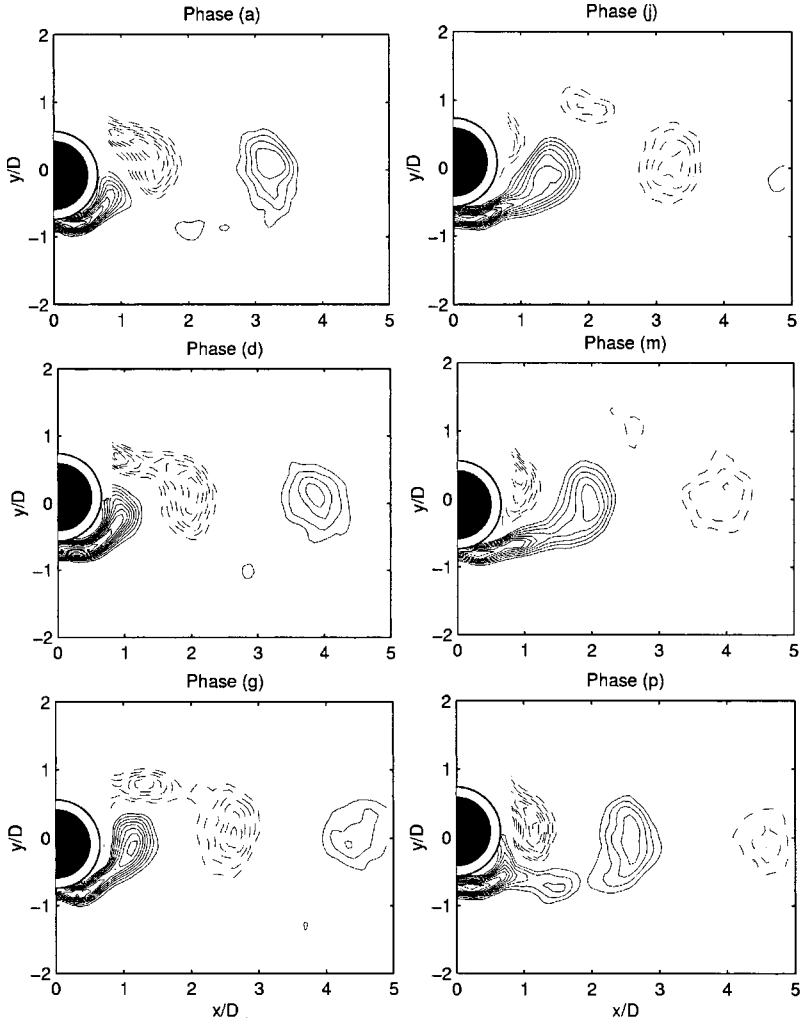

Fig. 9 Sequence of phase averaged vorticity fields for forced oscillating cylinder at $St_c=0.58$, $A/D=0.1$ (Case IV). ($|\langle\omega_z\rangle D/U_\infty|\rangle 1.0$, contour increment 0.5). See Fig. 13(*D*) for phase corresponding to each letter.

is generated in two cylinder oscillation, and a second smaller vortex is generated which does not appear to merge with the larger vortex in the near wake (Fig. 9).

In this study, a lack of synchronization of the wake with the cylinder oscillation is associated with roll-up of the vortices far downstream of the cylinder. For Case III and VI, the wake is not synchronized with the motion of the cylinder. The PSD of Case III, computed from the time-trace of u_y (transverse velocity) at the location of maximum fluctuations on the wake centerline, shows that the dominant frequency in the wake is at $St=0.20$ (Fig. 10). The Strouhal number, St, is defined as $St=fD/U_\infty$, where f is the wake frequency. The cylinder is oscillated at $St_c=0.34$, but there is little sign of wake excitation at the frequency of oscillation ($St_c=0.34$) in the PSD. This suggests that the shedding of the large-scale vortices is unaffected by the cylinder oscillation and remains near the frequency of the stationary cylinder at St ≈ 0.20. A sequence of the phase averaged vorticity field locked to the mechanical oscillation of the cylinder shows that the vorticity field at each phase looks remarkably like the mean vorticity field (Fig. 11(*A*)). This further confirms that the large-scale vortex shedding is unaffected by the cylinder oscillation at this oscillation frequency. By phase averaging with respect to u_y as described in the phase averaging section, the large-scale vortex shedding cycle can be recovered as shown in Fig. 11(*B*). The same behavior is observed for Case VI which has higher amplitude of $A/D=0.2$.

While a lack of synchronization of the wake with the mechanical oscillation of the cylinder results in vortices rolling-up far from the cylinder, a simple synchronization of the wake is *not* a sufficient condition to cause the vortices to roll-up close to the cylinder, i.e., high heat transfer. Figures 12(*A*) and (*B*) show the

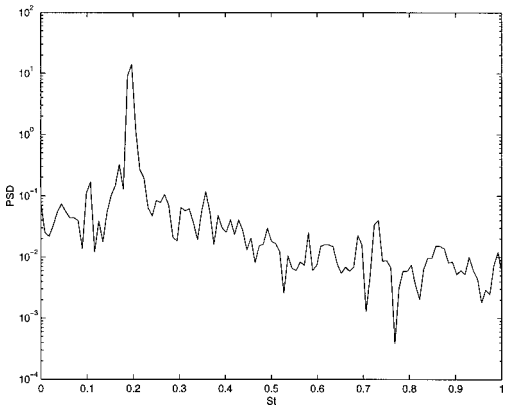

Fig. 10 PSD of u_y at location of maximum u_y fluctuations on the wake centerline for forced oscillating cylinder at $St_c=0.34$, $A/D=0.1$ (Case III)

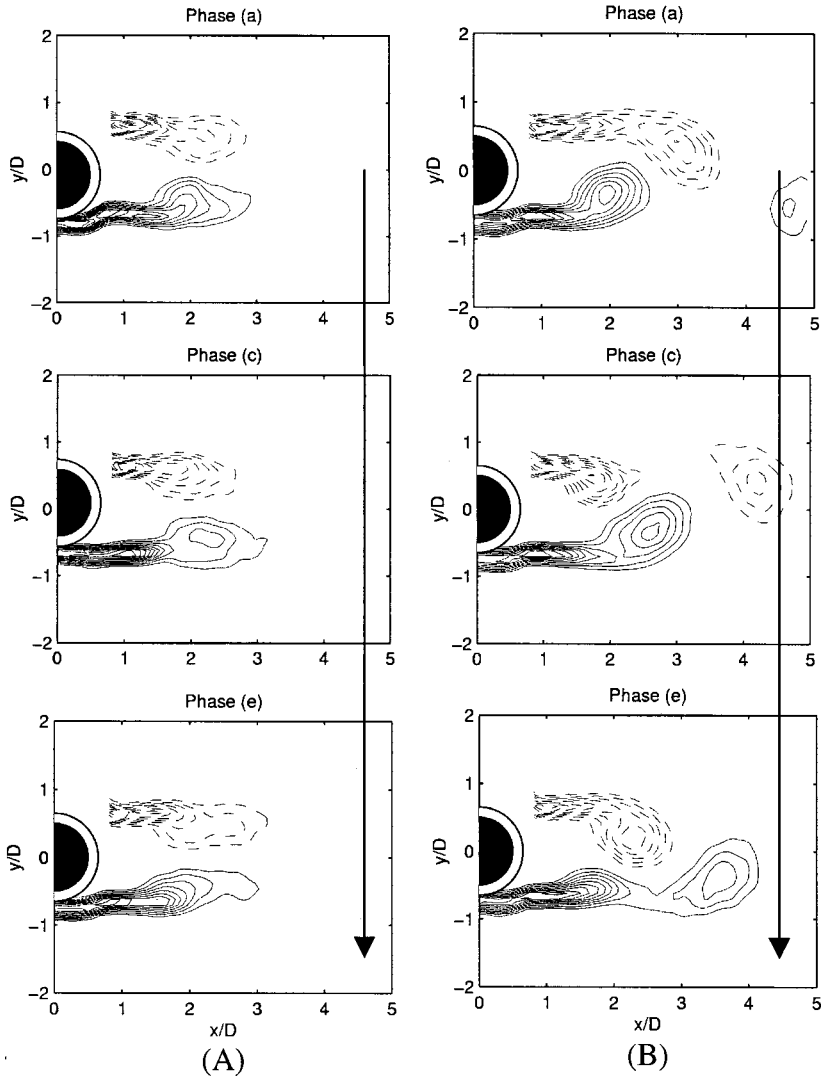

Fig. 11 Sequence of phase averaged vorticity fields for forced oscillating cylinder at $St_c=0.34$, $A/D=0.1$ (Case III). ($|\langle\omega_z\rangle D/U_\infty|$1.0, contour increment 0.5). The phase averaging is done with respect to the cylinder oscillation frequency in (*A*) and u_y at location of maximum u_y fluctuations on the wake centerline in (*B*). See Fig. 13(*A*) and (*B*) for phase corresponding to each letter.

wake patterns are synchronized with the one-half the cylinder oscillation frequency for both Cases VII and VIII, respectively. However, in Case VIII, which is of only slightly higher frequency, the vortices roll-up farther downstream as compared to Case VII, and this case has a low effective heat transfer rate.

Finally, the oscillation frequencies corresponding to the peaks in the heat transfer rate seem to shift slightly as function of oscillation amplitude. For $A/D=0.2$, the oscillation frequencies corresponding to the maximum heat transfer rates seem to shift lower than the multiples of the vortex shedding frequency of the unforced cylinder (Fig. 4). For smaller amplitude ($A/D=0.1$), the maximum heat transfer rate seem to nearly coincide with the multiples of the vortex shedding frequency of the unforced cylinder. Oddly, no peak in the heat transfer rate is observed for $A/D=0.1$ at twice the large-scale vortex shedding frequency. This is consistent with the results of Gau et al. [8] which also showed an increase at *only* three times the shedding frequency for $A/D<0.064$. While the results from Case III do not show any synchronization of the wake pattern with the oscillation frequency, the oscillation frequency may be too low ($St_c=0.34$). It is likely that the wake achieves synchronization at $St_c\approx0.4$ but probably fails to generate a pattern where the vortices roll-up close to the cylinder. Analogously, the heat transfer does not increase for oscillations frequencies corresponding to four or five times the large-scale vortex shedding frequency. The reason for why the wake has certain preferred frequencies at which the vortices roll-up close to the cylinder is unknown at this time.

''Turbulence'' Effect

From the results, we attempt to address the ''turbulence'' effect as described by Cheng et al. [4] who attributed it to the rise in heat transfer at $A/D=0.314$ past $St_c\approx0.3$. The ''turbulence'' effect, as it turns out, appears to be an organized pattern in the wake associated with the synchronization of the wake with the cylinder oscillation through processes of period doubling and tripling. For $A/D>0.2$, the increase in the heat transfer just above the natural vortex shedding frequency is associated with period doubling and is the result of vortices rolling-up closer to the cylinder and scrubbing away the stagnant fluid at the base of the cylinder for selected oscillation frequencies. At the lower amplitudes $A/D<0.1$, the heat transfer decreases because the vortices roll-up

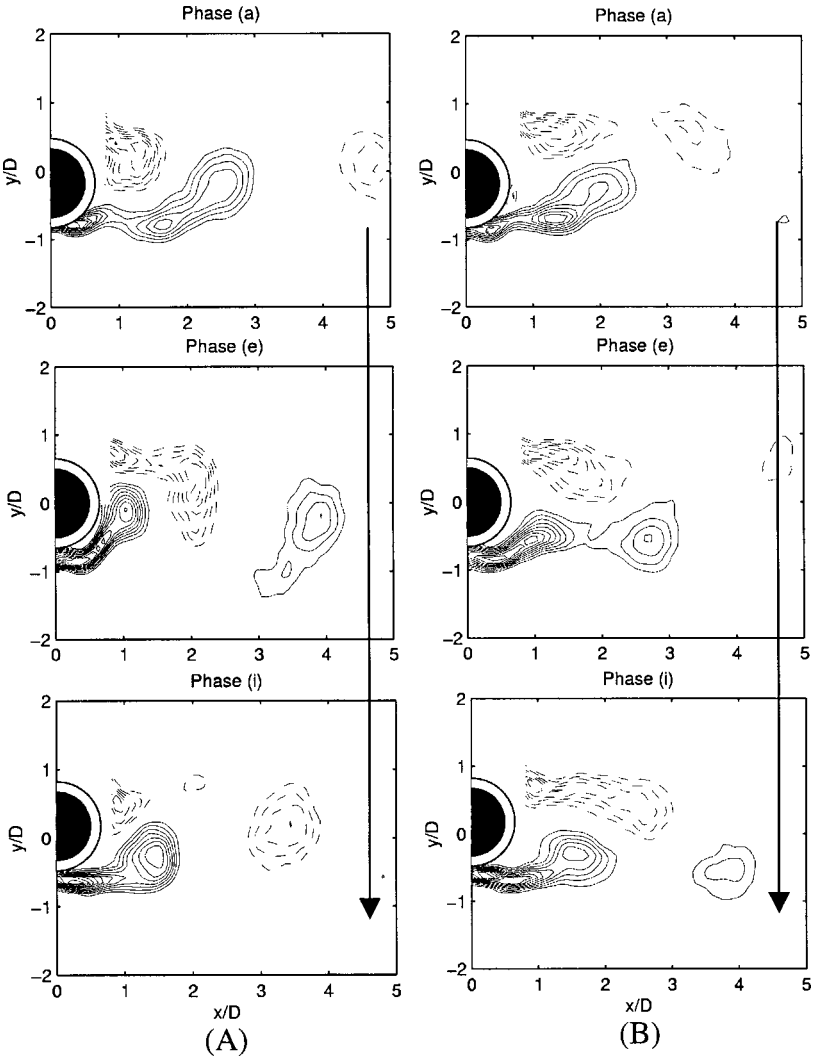

Fig. 12 Sequence of phase averaged vorticity fields for forced oscillating cylinder at $St_c=0.37$, $A/D=0.2$ (Case VII) (*A*), and $St_c=0.42$, $A/D=0.2$ (Case VIII) (*B*). ($|\langle\omega_z\rangle D/U_\infty|>1.0$, contour increment 0.5). See Fig. 13(*C*) for phase corresponding to each letter.

close to the cylinder only for three times the vortex shedding frequency. This result is confirmed by measurements by Gau et al. [8] for $A/D<0.064$. There may be indeed an effect from incoherent or ''turbulent'' motions in the wake as suggested by the result of Nusselt number never quite returning to the value of the stationary cylinder (Figs. 3 and 4, and Gau et al. [8]). However, the large increases observed at particular frequencies are the result of coherent or synchronized motion of the wake with respect to the cylinder oscillation.

Error Analysis

The relative uncertainty in the Nusselt number is given by:

$$\frac{\delta \mathrm{Nu}}{\mathrm{Nu}}=\left(\left[\frac{\delta(T_{tc}-T_\infty)}{(T_{tc}-T_\infty)}\right]^2+\left(\frac{\delta \dot{Q}}{\dot{Q}}\right)^2+\left(\frac{\delta D}{D}\right)^2+\left(\frac{\delta L}{L}\right)^2+\sum_{i=1}^{2}\left(\frac{\delta R_i}{R_i}\right)^2+\left(\frac{\delta k}{k}\right)^2+\left(\frac{\delta k_{CO}}{k_{CO}}\right)^2+\left(\frac{\delta k_{CI}}{T_{CI}}\right)^2\right)^{1/2}. \tag{12}$$

The relative uncertainty in the Nusselt number is on the order of 10 percent. The absolute uncertainty is roughly 25 percent. The large absolute uncertainty in Nusselt number comes using one-dimensional approximation of the surface temperature. A two-dimensional simulation shows that one-dimensional approximation produces a somewhat large bias error, i.e., absolute uncertainty, but the relative error is less sensitive. In other words, Nu_o may be off, but $\mathrm{Nu}/\mathrm{Nu}_o$ is accurate. Irrespective of our results, there is a large scatter in the Nusselt number found in literature. Again, one cause of the scatter might be the cylinder aspect ratio (L/D). It has been observed that decreasing the aspect ratio increases the wake bubble length; hence, the distance at which the vortices roll-up (Norberg [16]; Noca et al. [15]). Since the distance at which vortices roll-up plays an important role in the surface heat transfer when the cylinder is oscillated, the aspect ratio may be an important parameter in determining the relative increase in the heat transfer between a stationary and oscillated cylinder. Review of the aspect ratios used in previous studies show a range of rather low values, from $L/D=3$ of Saxena and Laird [20], $L/D=10.7$ of Kezios and Prasanna [11], $L/D=16$ of Cheng et al. [4], $L/D=17$ of Gau et al. [4], to $L/D=17.5$ for Sreenivasan and Ramachandran [21]. The end boundary conditions of these experiments have not been well documented. Therefore, the measurements from these studies, as well as the present study, may not be truly representative of heat transfer from an ''infinitely long'' circular cylinder which may be achieved only

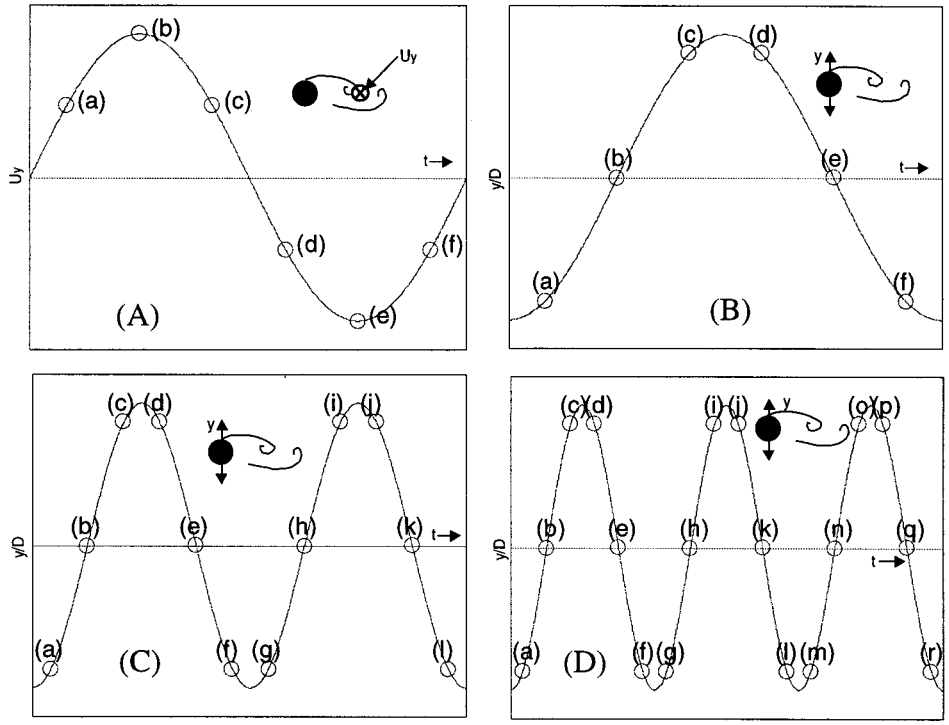

Fig. 13 Reference velocity and displacement of the cylinder corresponding to each letter of phase average

Table 1 Parameters from different studies

Authors	Re	Medium	A/D	Max. Nu/Nu_o	$Nu_o / Re^{0.5}Pr^{0.33}$	T_c-T_∞	L/D
Sreenivasan and Ramachandran (1961)	5,000-25,000	Air	0.43-3.7	≈1.0	≈0.5-0.7	≈75 °C	18
Kezios and Prasanna (1966)	5,500-14,000	Air	0.02-0.075	≈1.2	???	≈85 °C	11
Saxena and Laird (1978)	3,500	Water	0.89-1.99	≈1.6	???	≈9 °C	3
Cheng et al. (1997)	200-1000	Air	0.14-0.63	≈1.3	≈0.55	≈65 °C	16
Gau et al. (1999)	1600-4800	Air	0.064-0.016	≈1.4	≈0.55	???	17
Present Study	550-3500	Water	0.1-0.2	≈1.6	≈0.4-0.5	≈10 °C	13

when $L/D>50(200<\mathrm{Re}<1000)$ and $L/D>200$ for $\mathrm{Re}>1000$ (Norberg [16]). Thus there may not be a ''universal'' Nusselt number for a given Reynolds number. The parameters and results of each study are shown in Table 1.

A review of the previous measurements shows that there is a wide scatter in the measured heat transfer increase at the wake synchronization frequency ($\mathrm{St}_c \approx 0.2$). Experimentally, Kezios and Prasanna [11] measured increase of 20 percent for $A/D=0.075$ at $\mathrm{Re}=5500$, while Cheng et al. [4] measured increase of 10 percent for $A/D=0.138$ at $\mathrm{Re}=1000$ Gau et al. [8] has found increase up to 40 percent for $A/D=0.064$ at $\mathrm{Re}=1600$. There are some possible reasons for these discrepancies. First, some experiments were conducted in water and others in air, thus there may be Prandtl number effects. Second, each study used a different technique of computing the Nusselt number. Kezios and Prasanna [11] used thermocouples on the surface of a cylinder which was heated continuously, and the Nusselt number was estimated from the continuous power input and the average surface temperature. Gau et al. [8] made measurements similar to Kezios and Prasanna [11] except the heater strips were used to measure local Nusselt number. Cheng et al. [4] used thermocouples embedded within a cylinder which was first heated then allowed to cool by convection. The Nusselt number was computed indirectly by measuring the cooling rate of the cylinder. In this study, the cylinder is continuously heated, but the Nusselt number is computed using an *estimate* of the surface temperature from a thermocouple embedded in the cylinder core and the power input. It can be argued that the methods of Kezios and Prasanna [11] and Gau et al. [8] are the most accurate since they are the most direct measures of the Nusselt number. The results of this study are closer to those of Gau et al. [8] than those of Kezio and Prasanna [11] and Cheng et al. [4], but the issue is far from resolved. Since the cylinder used in this study was primarily designed for DPIV/T measurements, the computed Nusselt numbers in this study is not precise enough to address this question. However, the observed trends in the heat transfer rate as function of oscillation frequency and amplitude in this study are believed to be completely accurate.

Conclusion

In this study, we examine the effect of forced transverse oscillations on the heat transfer from the surface of a circular cylinder for $\mathrm{Re}=550$, 1100, 3500. A map is made of the heat transfer versus forced oscillation frequency for oscillation amplitudes, $A/D=0.1$ and 0.2. It is found that besides the increase in heat transfer at the oscillation frequency corresponding to the unforced vortex shedding frequency, there are other higher frequencies, namely super-harmonics, at which there is a large increase in the heat transfer. In particular, there is a large increase in heat transfer at approximately three times the unforced vortex shedding frequency for $A/D=0.1$, and there are large increases at approximately two and three times the frequency for $A/D=0.2$. A close inspection of the flow field using DPIV/T reveals that the increase in the heat transfer from a forced oscillating cylinder is linked with the distance at which vortices roll-up behind the cylinder. When the vortices roll-up close to the cylinder, the heat transfer is increased as the result of the removal of the stagnant and low heat convecting fluid at the base of the cylinder when the vortices approach close to the cylinder. The close roll-up of the vortices coincides with the synchronization of the wake with the mechanical oscillation of the cylinder through period doubling and/or tripling of the wake pattern with respect to the cylinder oscillation period. However, the synchronization of the wake with the mechanical oscillation is not found to be a sufficient condition to cause a large increase in the surface heat transfer. Only when the wake is synchronized and the vortices roll-up close to the cylinder, is a large increase in the surface heat transfer observed. Finally, the large increases in the heat transfer appear to be the result of coherent motions of the wake, not ''turbulent'' or incoherent motions.

Acknowledgments

We thank David Jeon and Dr. Flavio Noca for their generous help. This research was supported by NSF Grant CTS-9418973.

Nomenclature

A = amplitude of oscillation
Bi = Biot number (hD/k)
C_p = heat capacity
D = diameter of cylinder
f = frequency
f_c = frequency of cylinder oscillation
Gr = Grashof number ($g\beta(T_c-T_\infty)D^3/\nu^2$)
g = acceleration of gravity
h = convection heat transfer coefficient
k = thermal conductivity
k_{CO} = thermal conductivity of outer shell of cylinder
k_{CI} = thermal conductivity of heat coil inside cylinder
L = span of cylinder
Nu = Nusselt number (hD/k)
Nu_o = Nusselt number of stationary cylinder
Pr = Prandtl number (ν/α)
$\dot{Q}$ = heat input
$\dot{q}$ = heat input per unit mass
R_1 = inner radius of heating coil inside cylinder
R_2 = outer radius of heating coil inside cylinder
R_3 = outer radius of cylinder
Re = Reynolds number ($U_\infty D/\nu$)
St = Strouhal frequency (fD/U_∞)
St_c = Strouhal frequency of cylinder (f_cD/U_∞)
T = temperature
T_∞ = freestream temperature
T_c = surface temperature of cylinder
T_{tc} = temperature of thermocouple inside cylinder
t = time
U_∞ = freestream velocity
$\vec{u}$ = velocity vector
u_i = i^{th} velocity component
V_e = effective velocity of cylinder
V_v = RMS of transverse velocity of oscillating cylinder

Greek

α = heat diffusion coefficient ($k/\rho C_p$)
β = coefficient of thermal expansion
ρ = density
ν = kinematic viscosity
ω = vorticity

References

[1] Bearman, P. W., 1969, ''On Vortex Shedding From a Circular Cylinder in the Critical Reynolds Number Regime,'' J. Fluid Mech., **37**, pp. 577–586.
[2] Bloor, S., 1964, ''The Transition to Turbulence in the Wake of a Circular Cylinder,'' J. Fluid Mech., **19**, pp. 290–304.
[3] Cantwell, B., and Coles, D., 1983, ''An Experimental Study of Entrainment and Transport in the Turbulent Near Wake of a Circular Cylinder,'' J. Fluid Mech., **136**, pp. 321–374.
[4] Cheng, C. H., Chen, H. N., and Aung, W., 1997, ''Experimental Study of the Effect of Transverse Oscillation on Convection Heat Transfer From a Circular Cylinder,'' Journal of Heat Transfer, **119**, pp. 474–482.
[5] Cheng, C. H., and Hong, J. L., 1997, ''Numerical Prediction of Lock-On Effect on Convective Heat Transfer From a Transversely Oscillating Circular Cylinder,'' Int. J. Heat Mass Transf., **40**, pp. 1825–1834.
[6] Dabiri, D., and Gharib, M., 1991, ''Digital Particle Image Thermometry: The Method and Implementation,'' Exp. Fluids, **11**, pp. 77–86.
[7] Eckert, E. R. G., and Soehngen, E., 1952, ''Distribution of Heat Transfer Coefficients Around Circular Cylinder in Crossflow at Reynolds Numbers From 20 to 500,'' Trans. ASME, **74**, pp. 343–347.
[8] Gau, C., Wu, J. M., and Liang, C. Y., 1999, ''Heat Transfer Enhancement and Vortex Flow Structure Over a Heated Cylinder Oscillating in the Crossflow Direction,'' ASME Journal of Heat Transfer, **121**, pp. 789–795.
[9] Karanth, D., Rankin, G. W., and Sridhar, K., 1994, ''A Finite Difference

Calculation of Forced Convective Heat Transfer From an Oscillating Cylinder,'' Int. J. Heat Mass Transf., **37**, pp. 1619–1630.
[10] Karniadakis, G. E., 1997, private communication, Brown University, Providence, RI.
[11] Kezios, S. P., and Prasanna, K. V., 1966, ''Effect of Vibration on Heat Transfer From a Cylinder in Normal Flow,'' ASME Paper 66-WA/HT-43.
[12] Martinelli, R. C., and Boelter, L. M. K., 1938, ''The Effect of Vibration on Heat Transfer by Free Convection From a Horizontal Cylinder,'' *Proceedings of 5th International Congress of Applied Mechanics*, p. 578.
[13] Matsumura, M., and Antonia, R. A., 1993, ''Momentum and Heat Transport in the Turbulent Intermediate Wake of a Circular Cylinder,'' J. Fluid Mech., **250**, pp. 651–668.
[14] McAdams, W. H., 1954, *Heat Transmission*, McGraw-Hill, New York, p. 260.
[15] Noca, F., Park, H. G., and Gharib, M., 1998, ''Vortex Formation Length of a Circular Cylinder ($300<Re<4{,}000$) Using DPIV,'' *Proceedings of ASME Fluids Engineering Division Summer Meeting*, Paper FEDSM 98-5149.
[16] Norberg, C., 1994, ''An Experimental Investigation of the Flow Around a Circular Cylinder: Influence of Aspect Ratio,'' J. Fluid Mech., **275**, pp. 258–287.
[17] Ongoren, A., and Rockwell, D., 1988, ''Flow Structure From an Oscillating Cylinder Part 1. Mechanisms of Phase Shift and Recovery in the Near Wake,'' J. Fluid Mech., **191**, pp. 197–223.
[18] Park, H. G., 1998, ''A Study of Heat Transport Processes in the Wake of a Stationary and Oscillating Circular Cylinder Using Digital Particle Image Velocimetry/Thermometry,'' Ph.D. thesis, California Institute of Technology, Pasadena, CA.
[19] Roshko, A., 1993, ''Perspectives on Bluff Body Aerodynamics,'' J. Wind. Eng. Ind. Aerodyn., **49**, pp. 79–100.
[20] Saxena, U. C., and Laird, A. D. K., 1978, ''Heat Transfer From a Cylinder Oscillating in a Cross-Flow,'' ASME J. Heat Transfer, **100**, pp. 684–689.
[21] Sreenivasan, K., and Ramachandran, A., 1961, ''Effect of Vibration on Heat Transfer From a Horizontal Cylinder to a Normal Air Stream,'' Int. J. Heat Mass Transf., **3**, pp. 60–67.
[22] Taneda, S., 1956, ''Experimental Investigation of the Wakes Behind Cylinders and Plates at Low Reynolds Numbers,'' J. Phys. Soc. Jpn., **11**, p. 302.
[23] Willert, C. E., and Gharib, M., 1991, ''Digital Particle Image Velocimetry,'' Exp. Fluids, **10**, pp. 181–193.
[24] Williamson, C. H. K., and Roshko, A., 1988, ''Vortex Formation in the Wake of an Oscillating Cylinder,'' J. Fluids Struct., **2**, pp. 355–381.